

# Relaxation behaviours in ferromagnetic monolayers

*Ishita Tikader<sup>a</sup> and Muktish Acharyya<sup>b</sup>*

<sup>1</sup>Department of Physics, Presidency University,  
86/1 College Street, Kolkata-700073, India.

<sup>a</sup>E-mail:ishita.rs@presiuniv.ac.in

<sup>b</sup>E-mail: muktish.physics@presiuniv.ac.in

## Contents

<b>1</b>	<b>Introduction</b>	<b>3</b>
<b>2</b>	<b>Classic Mean-field theory of relaxation in Ising ferromagnet</b>	<b>4</b>
<b>3</b>	<b>Ferromagnetic Ising Model and Monte Carlo simulation scheme</b>	<b>6</b>
<b>4</b>	<b>Monte Carlo Simulational results</b>	<b>7</b>
4.1	Effects of geometry, boundary conditions and dynamics on magnetic relaxation .	7
4.1.1	Area non-preserving deformation . . . . .	10
4.1.2	Area preserving deformation . . . . .	12
4.1.3	Temporal Growth of Spin flip density . . . . .	13
<b>5</b>	<b>Experimental results of magnetic relaxation</b>	<b>19</b>
5.1	Critical slowing down . . . . .	19
<b>6</b>	<b>Summary:</b>	<b>21</b>
<b>7</b>	<b>Acknowledgements:</b>	<b>21</b>
<b>8</b>	<b>References</b>	<b>22</b>

arXiv:2305.10765v1 [cond-mat.stat-mech] 18 May 2023

**Abstract:** In this article, we briefly review the studies on magnetic relaxation behaviours. The theoretical as well as experimental investigations are reported briefly. A major part of this article is devoted to the recent Monte Carlo investigations into the roles of boundary conditions, dynamics and the Geometrical structures on the relaxation of magnetic monolayers modelled by two-dimensional Ising ferromagnet. We have studied all these effects for a two dimensional Ising system with two types of deformations, namely preserving and area non-preserving. The Glauber protocol and Metropolis dynamical rules are employed in our simulations and we investigated the systems with both periodic and open boundary conditions. The major findings are the exponential relaxation and the dependence of relaxation time ( $\tau$ ) on the aspect ratio  $R$  (length over breadth). A power law dependence ( $\tau \sim R^{-s}$ ) has been observed for larger values of aspect ratio ( $R$ ). The linear thermal ( $T$ ) dependence of exponent ( $s$ ) has been noticed ( $s = aT + b$ ). The transient behaviours of the spin-flip density have also been studied here for both surface and bulk/core. Both the saturated bulk/core and saturated surface spin-flip density are observed to follow the logarithmic dependence  $f_d = a + b \log(L)$  with the system size ( $L$ ). For open boundary condition with any kind (Metropolis/Glauber) of dynamical rule, the faster relaxation has been observed. Similarly, Metropolis algorithm yields faster relaxation for any kind (open/periodic) of boundary condition. We appeal to the experimentalists for experimental support which may be applied in judicious *magnetic coating* of the credit cards for quicker response.

**Keywords:** Ising model, Ferromagnetic system, Relaxation behaviour, Metropolis algorithm, Glauber dynamics, Monte Carlo simulation, spin-flip density, critical slowing down, critical exponents

### Objectives:

- The theoretical formulation of magnetic relaxation.
- Simulational results of relaxation of magnetic monolayers.
- How does the relaxation depend on the geometry of the system ?
- What are the roles of boundary conditions and dynamical rules ?
- How does the relaxation get accompanied by spin flips ?
- To have an idea about the real life magnetic relaxation.
- Technological significance of magnetic coating

# 1 Introduction

The relaxation phenomenon is ubiquitous in many physical systems. Particularly, the many-body systems in contact with a heat bath show variety of interesting relaxation behaviour depending on the temperature of the system. The thermodynamic systems, interacting cooperatively, show relaxation behaviour as they strive to achieve the equilibrium state. If the system is disturbed by an external perturbation (say magnetic field, electric field, stress etc.), it takes some time to restore the original equilibrium state, after the removal of the external perturbation. This relaxation behaviour in ferromagnetic systems is a well-celebrated field of research. The magnetically perturbed ferromagnetic systems relax (Slichter C. P 2020) towards their original equilibrium state, after the removal of the magnetic field. This relaxation behaviour of the ferromagnetic materials became an interesting field of study in the last few decades, both theoretically as well as experimentally.

Let us mention here some of the experimental studies on the relaxation of magnetic samples. The magnetic relaxation of the surface was studied in  $He^3$  experimentally (Godfrin et. al, 1980) by applying the technique of Nuclear Magnetic resonance in a confined geometry. The superconducting  $YBa_2Cu_3O_7$  sample has been used to study the magnetic relaxation, experimentally (Zazo et. al., 1993). The magnetic relaxation has been studied experimentally in a carbon nanotube-based magnetic nanocomposite sample (Rosa et. al, 2019). The single-ion magnets (Chiesa et. al., 2020) and single molecule magnets (Gu et. al., 2020) also show interesting magnetic relaxation. The non-Arrhenius (does not obey Neel-Arrhenius law) magnetic relaxation was also investigated (Suran et. al, 1998) experimentally. The micron sized ferromagnetic sample was used to study the relaxation behaviour (Klein et. al, 2003).

How can one investigate the magnetic relaxation in a simple ferromagnetic monolayer? The monolayer can be imagined as a two-dimensional ferromagnetic system. The simplest choice may be the spin-1/2 Ising ferromagnet. The Ising model is the prototype of ferromagnets. The relaxation behaviour of Ising ferromagnet (Richards, 1969) is exhaustively investigated in the recent past. The Ising ferromagnet does not have any intrinsic dynamics (governed by the Heisenberg equation of motion). However, the mean-field dynamical equation was developed (Suzuki and Kubo, 1968) for Glauber kinetic (Glauber 1963) Ising ferromagnet. This mean-field dynamical equation may be employed as the simple model to study the dynamical phenomena, e.g. relaxation behaviour.

To have an idea about the importance of Ising model to study the relaxation behaviour, a few important studies (related to relaxation behaviour) are mentioned here. How can the spin-spin correlation decay in time? The temporal decay of spin-spin correlation (in the low temperature regime) in the one-dimensional Ising ferromagnet has been studied (Brey and Prados 1996) using Glauber dynamics. The large scale critical dynamics have been focussed (Lin and Wang 2016) to study the linear relaxation in two-dimensional Ising ferromagnet and to estimate the dynamic exponent. The energy-relaxation in two dimensional Ising model has been studied (Mori 1993) by Monte Carlo simulation and estimated the critical exponents (above critical temperature) of linear and nonlinear relaxations of the internal energy. The Pade approximation method has been employed to study the linear and nonlinear relaxation behaviour in kinetic Ising model (Collins et. al., 1987). The interesting tricritical relaxation was investigated (Muller-Krumbhaar and Landau 1976) in Glauber kinetic three-dimensional Ising model and found the exponential relaxation below the tricritical temperature. A peculiar slow relaxation has been reported recently (Jeong et. al, 2005) in the small-world networks of Ising model with strong long-range interactions. The critical nonequilibrium relaxation in Ising model has also been studied (Tomita and Nonomura 2018).

Tomita and Miyashita (1992) studied the field and size dependence of the relaxation behaviour of the metastable states of the two dimensional Ising model. The speed of relaxation is important in the relaxation dynamics of magnetic system. The slow relaxation (in a constrained Ising spin chain) has been reported (Majumdar and Dean 2002). In the nonequilibrium relaxation of the Ising model, a comparison has been studied (Wang and Gan 1998) for Monte Carlo method and series expansion.

The relaxation behaviour of Glauber kinetic Ising model has been studied (Binder et. al., 1975) in the

context of the dynamics and clusters near the critical point. The disorder or the nonmagnetic-impurities plays an important role in the relaxation of magnetic system. Keeping this in mind, the effects of random impurities on the relaxation of Ising ferromagnets have also been investigated (Oerding 1995). What kind of distribution of relaxation time is expected if it is recorded for different samples ? This is an important question in the context of statistical mechanical problems. The statistical distribution of the relaxation times (recorded in different samples of Ising ferromagnet) has been studied (Melin 1996) and found that in the strong field regime, the logarithm of the relaxation time is normally distributed. The relaxation in Ising model has been investigated (decay of Hamming distance by Monte Carlo simulations) in the context of damage spreading and observed (Grassberger and Stauffer 1996) a simple exponential decay in three and four dimensions both below and above the Curie temperature. In two dimensions, a stretched exponential decay is observed only below the critical temperature. The research on the relaxation behaviour of Ising ferromagnet is not only limited by spin- 1/2 . It would be interesting to know the relaxation behaviours in the case of higher values of the spin. The magnetic relaxation in spin-1 Ising ferromagnet has also been studied (Erdem 2008) near the second-order phase transition point by solving the (molecular) field theoretically derived kinetic equation. They have obtained the magnetic dispersion and calculated the absorption factor near the second-order phase transition point. What kind of relaxation behaviour is expected in the antiferromagnets ? Slow relaxation has been observed (Nowak and Usadel 1989) in diluted antiferromagnets by Monte Carlo simulation.

With this brief introduction to the relaxation behaviours in Ising model, we report some additional and interesting results of our recent work on the relaxation behaviour of Ising monolayer (two dimensional system) in different geometrical conditions. We also report some results on the dynamics dependence of the relaxation behaviour observed by Monte Carlo simulation. The boundary conditions and its role are also discussed in this article.

## 2 Classic Mean-field theory of relaxation in Ising ferromagnet

The relaxation of magnetisation was theoretically studied by M. Suzuki and R. Kubo for two and three-dimensional Ising model in the neighbourhood of critical point using mean-field approximation (Suzuki and Kubo, 1968). In order to understand the relaxation behaviours of Ising ferromagnet, it would be beneficial, to begin with a concise explanation of the concept.

Let us consider a system of interacting Ising spins (spin-1/2) which are represented by the spin variables,  $\{S_i\}$ .  $S_i$  can assume values  $\pm 1$  (for spin-1/2 system). The system interacts with a large isothermal heat bath at a fixed temperature  $T$ . Probability of spin-flip of  $i^{\text{th}}$  spin is denoted as  $W_i(S_i)$ . This is not only determined by  $S_i$ , but also influenced by the neighbouring spin variables. Following Suzuki and Kubo (Suzuki and Kubo, 1967) the Markovian dynamical master equation for this model can be written as

$$\frac{dP(S_1, S_2 \dots S_i \dots S_N; t)}{dt} = - \sum_i W_i(S_i) P(S_1, S_2 \dots S_i \dots S_N; t) + \sum_i W_i(-S_i) P(S_1, S_2 \dots - S_i \dots S_N; t) \quad (1)$$

where  $P(S_1, S_2 \dots S_N; t)$  is the probability of finding the spins in the configuration  $(S_1, S_2, \dots, S_N)$ . The first summation term in the right-hand side of the equation-1 represents the loss of probability due to spin flipping out and the second one is the gain by flipping from the opposite direction. In thermal equilibrium,  $\frac{dP}{dt} = 0$ , the Principle of detailed balance is applicable in this context. So we have the equation,

$$W_i(S_i) P_{eq}(S_1, S_2 \dots S_i \dots S_N) = W_i(-S_i) P_{eq}(S_1, S_2 \dots - S_i \dots S_N) \quad (2)$$

where  $P_{eq}(S_1, S_2 \dots S_N)$  is the probability in equilibrium. So we can write,

$$\frac{W_i(S_i)}{W_i(-S_i)} = \frac{P_{eq}(S_1, S_2 \dots - S_i \dots S_N)}{P_{eq}(S_1, S_2 \dots S_i \dots S_N)} \quad (3)$$

In the presence of an external magnetic field, the energy of the Ising system is given by following Hamiltonian,

$$H = - \sum_{\langle i,j \rangle} J_{ij} S_i S_j - \sum_i h_i S_i \quad (4)$$

where the first term of the Hamiltonian represents the spin-spin interaction between the pair  $\langle ij \rangle$  and the second term arises due to the interaction with an externally applied magnetic field  $h_i$  (site dependent in general).

According to Gibbs canonical distribution, the probability of finding a system in a particular configuration C is,

$$P(C) = \frac{1}{Z} \exp(-\beta E_C) \quad (5)$$

Here  $\beta = 1/k_B T$  and  $E_C$  is the energy of the system in that particular configuration C. Here,  $k_B$  denotes the Boltzmann constant.

Detailed balanced condition (in equilibrium) ensures that,

$$\frac{W_i(S_i)}{W_i(-S_i)} = \frac{\exp(-\beta E_i S_i)}{\exp(\beta E_i S_i)} \quad (6)$$

where  $E_i$  is the local field energy defined by,

$$E_i = \sum_j J_{ij} S_j + h_i \quad (7)$$

Since Ising spins can possess only two discrete values +1 or -1, by the definition of Pauli spin matrices we can write the above-mentioned exponential terms in this form,

$$\exp(\pm\beta E_i S_i) = \cosh(\beta E_i) \pm S_i \sinh(\beta E_i) = \cosh(\beta E_i) [1 \pm S_i \tanh(\beta E_i)] \quad (8)$$

So, equation (6) can be written as,

$$\frac{W_i(S_i)}{W_i(-S_i)} = \frac{1 - S_i \tanh(\beta E_i)}{1 + S_i \tanh(\beta E_i)} \quad (9)$$

From the Glauber prescription (Glauber, 1963) we can express the transition probability as,

$$W_i(S_i) = \frac{1}{2\tau_m} (1 - S_i \tanh(\beta E_i)) \quad (10)$$

Here  $\tau_m$  is a constant, called Microscopic Relaxation Time. It not only depends on the temperature but also on the neighbouring spins. To avoid unnecessary complexities we assume  $\tau$  depends on the temperature only.

The expectation value of the  $i^{\text{th}}$  spin is defined as

$$\langle S_i \rangle = \sum_{\{S_i\}} S_i P(S_1, S_2, \dots, S_i, \dots, S_N; t) \quad (11)$$

Now taking the total time derivative of  $\langle S_i \rangle$  We may write,

$$\frac{d\langle S_i \rangle}{dt} = \sum_{\{S_i\}} S_i \frac{dP(S_1, S_2, \dots, S_i, \dots, S_N; t)}{dt} \quad (12)$$

Using the Markovian master equation (equation-1) we can easily obtain the following differential equation:

$$\tau_m \frac{d}{dt} \langle S_i \rangle = -\langle S_i \rangle + \langle \tanh \beta E_i \rangle \quad (13)$$

The above differential equation can be easily solved with the simplest approximation, which corresponds to the mean-field theory. In this approximation above equation(13) can be replaced by,

$$\tau_m \frac{d}{dt} \langle S_i \rangle = -\langle S_i \rangle + \tanh(\beta \langle E_i \rangle) \quad (14)$$

where in the particular case of a homogeneous magnetic field,

$$\langle E_i \rangle = \sum_j J_{ij} \langle S_j \rangle + h \quad (15)$$

We may rewrite the equation (14) for instantaneous average magnetisation  $m(t)$  (where  $m = \langle S_i \rangle = \langle S_j \rangle$ );

$$\tau_m \frac{dm}{dt} = -m + \tanh \beta(h + \lambda m); \quad \lambda = \sum_j J_{ij} \quad (16)$$

In the absence of an external magnetic field ( $h = 0$ ) and in the neighbourhood of the Critical point, we can linearize the equation(16),

$$\begin{aligned} \tau_m \frac{dm}{dt} &= -\kappa m; \\ \text{where, } \kappa &= 1 - \beta \lambda = 1 - \frac{T_c}{T}; \\ T_c &= \frac{\lambda}{k_B}, \text{ Critical Temperature} \end{aligned} \quad (17)$$

Solving equation (17) we can interpret that, the relaxation of magnetisation at fixed temperature  $T$  will follow exponential law given by,

$$\begin{aligned} m(t) &\propto \exp\left(-\frac{\kappa}{\tau_m} t\right) \\ \tau_r &= \frac{\tau_m}{\kappa} = \frac{\tau_m T}{T - T_c} \end{aligned} \quad (18)$$

From the above equation we can obtain that,  $\tau_r \sim (T - T_c)^{-1}$ , where  $\tau_r$  is the macroscopic relaxation time. The diverging relaxation time near the critical temperature is called 'Critical slowing down'. The critical slowing down can be visualized from a simple mean-field differential equation of Kinetic Ising ferromagnet.

However, the thermodynamic fluctuations are ignored in the mean-field approximation. Thermodynamic fluctuation plays a major role in the ferro-para transition. To study the relaxation behaviours incorporating the thermodynamic fluctuations one has to employ a simple lattice model and the Monte Carlo method using dynamical algorithms. Moreover, the effects of the lattice geometry and the boundary conditions cannot be studied by simple mean-field dynamical equations. The Monte Carlo method can be simply applied to study these effects on the relaxation behaviours of Ising ferromagnets.

### 3 Ferromagnetic Ising Model and Monte Carlo simulation scheme

In the present chapter, our discussion is focussed on the Monte Carlo simulational studies of relaxation behaviours observed in ferromagnets, specifically investigating the discrete classical spin models, namely the Ising model. The Ising model is a well-established prototype for studying the behaviours of magnetic systems.

A two-dimensional Ising ferromagnetic system in the absence of any external magnetic field is modelled by the following Hamiltonian,

$$H = -J \sum_{\langle i,j \rangle} S_i S_j \quad (19)$$

where Ising spin variables  $S_i$  can have two discrete spin states ( $\pm 1$ ) i.e., the spin moment axis is either pointing up (+1) or down (-1).  $J$  is the uniform ferromagnetic interaction strength between the nearest neighbour spins only. The positive value of  $J$  ( $J > 0$ ) indicates the ferromagnetic behaviour of the system.

We have considered a two-dimensional rectangular lattice, where the total number of spins  $N = L_x \times L_y$ .  $L_x$  and  $L_y$  denote the length measured along X-axis and Y-axis respectively and for a square lattice,  $L_x$  and  $L_y$  must be equal (i.e.,  $L_x = L_y$ ). In order to study the impact of boundary conditions on relaxation behaviour, both periodic and open boundary conditions are employed in both directions.

Let us take a moment to summarize the Monte Carlo simulation protocol we have employed in our subsequent investigations. The initial system is considered to be in a perfectly ordered state where  $S_i = +1; \forall i$  due to the presence of a high external magnetic field. The system is in thermal equilibrium with a heat bath maintained at constant (nonzero) temperature  $T$ . Now the lattice sites will be updated by the 'random updating scheme'. We choose a lattice site (say  $i^{th}$ ) randomly and calculate the change in energy  $\Delta E$  due to a trial spin-flip ( $S_i \rightarrow -S_i$ ) governed by the Ising Hamiltonian (19). The probability of spin-flip at the targeted site is determined by either the 'Metropolis single spin flip algorithm' or the 'Glauber Dynamical algorithm' (depending on the specific topic under study).

According to the Metropolis algorithm (Metropolis 1953), the transition probability is given by,

$$P(S_i \rightarrow -S_i) = \text{Min}[1, \exp(-\frac{\Delta E}{k_B T})] \quad (20)$$

The Glauber transition probability is represented by,

$$P(S_i \rightarrow -S_i) = \frac{\exp(-\frac{\Delta E}{k_B T})}{1 + \exp(-\frac{\Delta E}{k_B T})} \quad (21)$$

$k_B$  is the Boltzmann constant and  $T$  is the temperature of the system measured in unit of  $J/k_B$ .  $\Delta E$  is measured in unit of  $J$ . For simplicity, we have assumed  $k_B = 1$  and  $J = 1$  throughout our simulation study.

Next, we compare the transition probability  $P(S_i \rightarrow -S_i)$  (Metropolis or Glauber) to a randomly generated number (say  $r$ ) which is uniformly distributed between 0 and 1. If the random number 'r' satisfies the following condition:  $r \leq P(S_i \rightarrow -S_i)$  only then the trial spin-flip would be accepted. Otherwise, the system remains in the initial spin state. A total of  $L_x \times L_y$  randomly chosen lattice sites are updated obeying the aforementioned protocol and 1 Monte Carlo Step per Spin or MCSS is completed, which serves as the unit of time throughout the simulation study. At each MCSS instantaneous magnetisation is defined by

$$m'(t) = \frac{1}{N} \sum_{i=1}^N S_i. \quad (22)$$

The average instantaneous magnetization  $m(t)$  is calculated over several different samples.

## 4 Monte Carlo Simulation results

### 4.1 Effects of geometry, boundary conditions and dynamics on magnetic relaxation

Initially, we have opted a square lattice of size  $L_x = L_y$ , where all spins are in the up-state; i.e.,  $S_i = +1; \forall i$ . This scenario can be visualised as that the system is perturbed by a strong external magnetic field along the positive  $z$  direction. After abruptly switching off the magnetic field, the system is no longer under the influence of the external field. It starts to relax toward its equilibrium state at a fixed temperature  $T > T_c$  (where  $T_c$  is the Critical temperature). We have studied the relaxation behaviour of a two-dimensional Ising ferromagnetic system and explored how this relaxation behaviour is impacted by the lattice geometry and

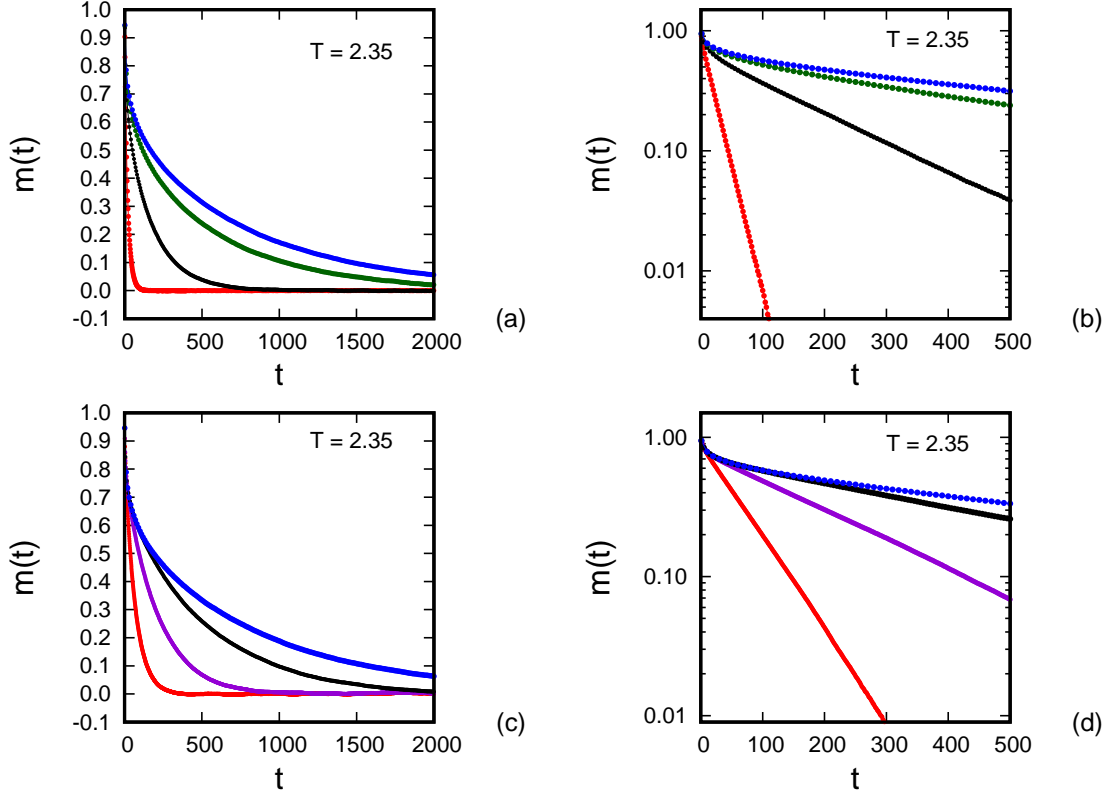


Figure 1: The temporal variations of magnetisation at temperature  $T = 2.35$  for different sizes of the system. In the case of a system with Open Boundary Condition, the graphical plots are represented for the following system sizes i.e. for fixed  $L_x = 512$ ,  $L_y = 512$  (Blue),  $L_y = 64$  (Green),  $L_y = 16$  (Black) and  $L_y = 4$  (Red). (a) In the linear scale and (b) in the logarithmic scale. In the case of a system with Periodic Boundary Condition the graphical plots are represented for the following system sizes i.e. for fixed  $L_x = 512$ ,  $L_y = 512$  (Blue),  $L_y = 16$  (Black),  $L_y = 8$  (Violet) and  $L_y = 4$  (Red). (c) In the linear scale and (d) in the logarithmic scale. Metropolis Algorithm has been employed here. Data are averaged over 10000-80000 samples (depending upon the size of the lattice). I Tikader, O. Mallick and M. Acharyya, arXiv:2212.01858v1.

boundary conditions (open or periodic). Furthermore, we have investigated the influence of the dynamical algorithms implemented here.

We have thoroughly observed the decay of the average magnetisation  $m(t)$  with time. The system is kept at a temperature  $T = 2.35$  i.e.; in the paramagnetic phase ( $T_c = 2.269\dots$  is the Onsager value). Therefore the magnetisation will eventually vanish. We have shown these results in Fig1 for different sizes (by changing  $L_y$  for a fixed value of  $L_x$ ) of the system for different boundary conditions. The Metropolis dynamical rule is employed here. Fig1(a) represents the magnetisation as a function of time for open boundary condition. The exponential nature of the decay of the magnetisation (i.e.,  $m(t) \sim e^{(-t/\tau)}$ ) is found by studying the logarithm of the magnetisation ( $\log(m)$ ) as a linear function of time. This is shown in Fig-1(b). The inverse of the slope of this linear function ( $\log(m) - t$ ) has been measured (by linear regression method) and identified as the relaxation time ( $\tau$ ) of the system. Similarly, the relaxation or decay of magnetisation with time has been studied using the periodic boundary conditions in both directions. Fig1(c) illustrates the decay of

magnetisation ( $m(t)$ ) with time. Here also, the relaxation time  $\tau$  has been measured from the linear fit of  $\log(m) - t$  as shown in the Fig1(d). The results are qualitatively similar for both the boundary conditions implemented here. A significant role of the boundary conditions is observed here for smaller values of  $L_y$ . It is evident that the relaxation is faster (comparing the results shown in Fig-1(b) and Fig-1(d)) in the case of open boundary conditions, where all other parameters are kept unchanged.

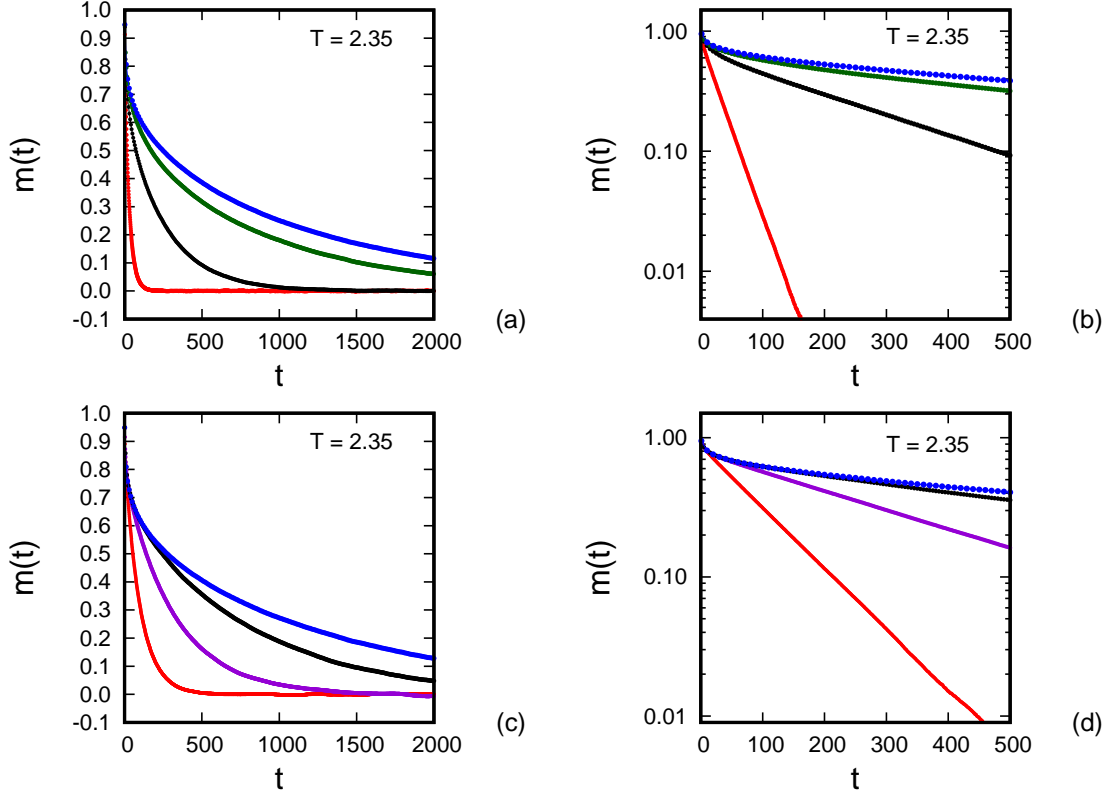


Figure 2: The temporal variations of magnetisation at temperature  $T = 2.35$  for different sizes of the system. In the case of a system with Open Boundary Condition, the graphical plots are represented for the following system sizes i.e. for fixed  $L_x = 512$ ,  $L_y = 512$  (Blue),  $L_y = 64$  (Green),  $L_y = 16$  (Black) and  $L_y = 4$  (Red). (a) In the linear scale and (b) In the logarithmic scale. In the case of a system with Periodic Boundary Condition, the graphical plots are represented for the following system sizes i.e. for fixed  $L_x = 512$ ,  $L_y = 512$  (Blue),  $L_y = 16$  (Black),  $L_y = 8$  (Violet) and  $L_y = 4$  (Red). (c) In the linear scale and (d) In the logarithmic scale. Glauber rule has been employed here. Data are averaged over 10000-80000 samples (depending upon the size of the lattice). This figure is collected from the paper authored by I Tikader, O. Mallick and M. Acharyya, arXiv:2212.01858v1.

What would be the relaxation scenario in the context of Glauber kinetic Ising ferromagnet? We have investigated the relaxation behaviour of magnetisation by employing the Glauber protocol with different boundary conditions. The results are demonstrated in Fig-2. Similarly, Figure 2(a) (linear scale) and Figure 2(b) (logarithmic scale) depict the results for the system with open boundary condition.

On the other hand, the results for periodic boundary conditions are shown in Fig-2(c) (linear scale) and Fig-2(d) (logarithmic scale). Here also, we have observed that the open boundary condition accelerates the

relaxation process. Qualitatively, we can say that in the case of open boundary conditions, the spins at the boundary has only three nearest neighbours on interactions in two dimensions. Whereas in the case of periodic boundary conditions, all the spins have four nearest interacting neighbours. As a result, the open boundary is more vulnerable to spin-flip leading to the faster relaxation.

It is also evident that the system using the Metropolis algorithm approaches the thermodynamic equilibrium faster than that compared to the system with Glauber dynamics. The reason behind this observation is quite clear as the Metropolis probability can assure the spin-flip (for negative change in energy due to flip) which is not provided by Glauber protocol. Consequently, the Metropolis algorithm promotes faster convergence to the thermodynamic equilibrium compared to the Glauber dynamics.

Our primary goal is to investigate whether the relaxation behaviour of the system remains consistent if we alter the geometrical structure of the lattice. Specifically, how does the relaxation time get affected when the square lattice is deformed into a rectangular one? We are concerned about both cases (i) area non-preserving deformation (reducing  $L_y$  and keeping  $L_x$  fixed) and (ii) area preserving deformation (with  $L_x \times L_y$  fixed).

#### 4.1.1 Area non-preserving deformation

In this study, we have gradually changed the geometry of the lattice and deformed the square lattice into a rectangular one just by reducing  $L_y$  and keeping  $L_x$  fixed. We have measured (Tikader, Mallick and Acharyya 2022) the instantaneous magnetisation ( $m(t)$ ) of the Ising ferromagnetic system for different lattice sizes by varying its length along the Y-axis,  $L_y = 512, 256, 128, 64, 32, 16, 12, 8, 6, 4, 3$  and  $2$  for a fixed value of  $L_x = 512$ . The aspect ratio of the lattice geometry is defined by  $R = \frac{L_x}{L_y}$ . We have observed the variation of the relaxation time ( $\tau$ ) with the aspect ratio ( $R$ ) under different boundary conditions and dynamical rules. Our results are demonstrated in a compact form in Fig-3.

The logarithm of the relaxation time ( $\log(\tau)$ ) is plotted as a function of the logarithm of the aspect ratio ( $\log(R)$ ). Fig-3(a) illustrates the results obtained using the Metropolis algorithm for the system with open boundary condition, while Fig-3(b) represents the results under periodic boundary condition. Similarly, the results obtained by applying Glauber dynamical rule are depicted in Fig-3(c) and Fig-3(d) for open and periodic boundary conditions respectively. We have demonstrated our findings for two different temperatures ( $T = 2.325$  and  $T = 2.400$ ). An interesting scenario is observed here. Across all cases, the relaxation time  $\tau$  exhibits a minimal sensitivity to aspect ratio( $R$ ), particularly for the smaller values of  $R$ . However for higher values of  $R$ , the relaxation time  $\tau$  appears to be significantly dependent on it. The plots clearly indicate that for the large  $R$  limit,  $\log(\tau)$  has linear dependence (found by linear regression) on  $\log(R)$ , having a negative value of the slope. This observation led us to propose a power law relation between  $\tau$  and  $R$  like  $\tau \sim R^{-s}$ . Our analysis suggests that the exponent  $s$  of this power law variation is also temperature dependent ( $s(T)$ ). As the temperature increases the value of the exponent  $s$  is found to decrease for any particular type of boundary condition and the dynamical rule. For any fixed temperature and boundary condition, the value of the exponent  $s$  is slightly larger for Glauber dynamics. For a particular type of dynamical rule and fixed temperature, the periodic boundary condition estimates a larger value of the exponent  $s$ .

In order to determine the specific thermal ( $T$ ) variation of the exponent  $s$ , we have performed a comprehensive analysis of the exponent  $s$  ( $\tau \sim R^{-s}$ ), across a range of temperatures within the paramagnetic region (close to  $T_c$ ). The obtained results are graphically represented in Fig-4. Fig-4(a) and Fig-4(b) depict the graphical plots of our findings using Metropolis algorithm for the system with open and periodic boundary conditions respectively. Similarly, the results obtained by the Glauber dynamical rule are presented in Fig-4(c) and in Fig-4(d) for open and periodic boundary conditions respectively. It is clearly observed that show that the exponent  $s$  linearly decreases with temperature, i.e.  $s = aT + b$ . The outcomes obtained by linear regression and the fit statistics are provided in Table-1. Both Metropolis and Glauber dynamics exhibit strikingly similar observations in qualitative terms. It is also remarkable that the rate of linear fall ( $-\frac{ds}{dT}$ ) of the exponent  $s$  with respect to the temperature is considerably higher for a system with periodic boundary condition.

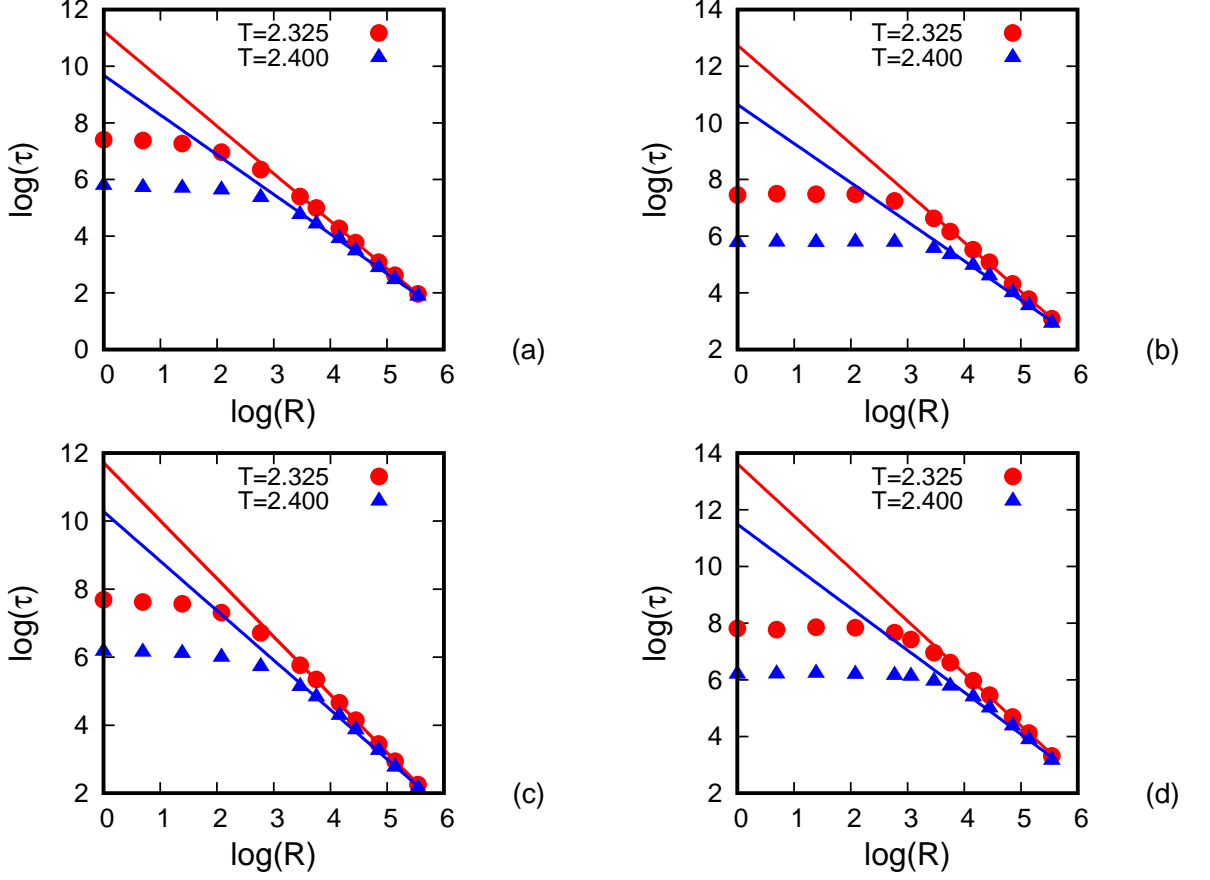


Figure 3: The logarithm of Relaxation time ( $\log(\tau)$ ) is plotted against the logarithm of the aspect ratio ( $\log(R = L_x/L_y)$ ) for two different temperatures in Para phase,  $T = 2.325$  (Red circle) and  $T = 2.400$  (Blue triangle). Both plots are fitted to the straight line function,  $\log(\tau) = -s \times \log(R) + r$ . (a) **For open boundary conditions and Metropolis dynamics:** At  $T = 2.325$ ;  $s = 1.67 \pm 0.02, r = 11.23 \pm 0.07$  (Red). Here  $\text{DOF} = 5$  and  $\chi^2 = 0.004$ . And at  $T = 2.400$ ;  $s = 1.40 \pm 0.02, r = 9.68 \pm 0.11$  (Blue). Here  $\text{DOF} = 5$  and  $\chi^2 = 0.009$ . (b) **For periodic boundary conditions and Metropolis dynamics:** At  $T = 2.325$ ;  $s = 1.74 \pm 0.03, r = 12.74 \pm 0.15$  (Red). Here  $\text{DOF} = 4$  and  $\chi^2 = 0.009$ . And at  $T = 2.400$ ;  $s = 1.38 \pm 0.06, r = 10.65 \pm 0.29$  (Blue). Here  $\text{DOF} = 4$  and  $\chi^2 = 0.033$ . (c) **For open boundary conditions and Glauber dynamics:** At  $T = 2.325$ ;  $s = 1.70 \pm 0.02, r = 11.72 \pm 0.07$  (Red). Here  $\text{DOF} = 5$  and  $\chi^2 = 0.004$ . And at  $T = 2.400$ ;  $s = 1.46 \pm 0.04, r = 10.28 \pm 0.17$  (Blue). Here  $\text{DOF} = 5$  and  $\chi^2 = 0.023$ . (d) **For periodic boundary conditions and Glauber dynamics:** At  $T = 2.325$ ;  $s = 1.85 \pm 0.04, r = 13.62 \pm 0.19$  (Red). Here  $\text{DOF} = 4$  and  $\chi^2 = 0.01$ . And at  $T = 2.400$ ;  $s = 1.48 \pm 0.08, r = 11.49 \pm 0.38$  (Blue). Here  $\text{DOF} = 4$  and  $\chi^2 = 0.06$ . This figure is collected from the paper authored by I Tikader, O. Mallick and M. Acharyya, arXiv:2212.01858v1.

Our results obtained under various dynamics and boundary conditions are summarized in a tabular form in Table-1.

**Table 1**

Dynamical rule	Boundary condition	$a$	$b$	$\chi^2$	DoF
Metropolis	Open	$-3.53 \pm 0.18$	$9.87 \pm 0.42$	0.0006	3
	Periodic	$-4.56 \pm 0.17$	$12.33 \pm 0.41$	0.0005	3
Glauber	Open	$-3.28 \pm 0.11$	$9.33 \pm 0.25$	0.0002	3
	Periodic	$-4.69 \pm 0.16$	$12.74 \pm 0.38$	0.0004	3

Table 1: Fitting parameters for exponent  $s$  versus temperature  $T$  plot (Area non-preserving deformation). Collected from I Tikader, O. Mallick and M. Acharyya, arXiv:2212.01858v1.

#### 4.1.2 Area preserving deformation

Now, if we transform the square lattice into a rectangular shape in such a way the area of the lattice remains constant, what would be the scenario? How does this area-preserving deformation (Tikader, Mallick and Acharyya 2023) impact the relaxation time  $\tau$ ? This is a very relevant question that deserves attention. In this context, we systematically changed the lattice geometry by deforming our initially chosen square lattice ( $L_x = L_y = 64$ ) into a rectangular one keeping its area  $L_x \times L_y$  fixed and thoroughly observed the time evolution of magnetisation  $m(t)$  for different lattice sizes of the system. We have taken its length along X-axis,  $L_x = 64, 128, 256, 512, 1024$  and  $2048$  and changed the corresponding values of  $L_y$  so that  $L_x \times L_y = 4096$ . We have investigated the dependence of relaxation time ( $\tau$ ) on the aspect ratio ( $R = \frac{L_x}{L_y}$ ) under different boundary (open and periodic) conditions using different dynamical rules (Metropolis and Glauber). Fig-5 depicts how the logarithm of relaxation time ( $\log(\tau)$ ) varies with the logarithmic values of aspect ratio ( $\log(R)$ ). Based on our observation, it is evident that in the higher regime of  $R$  a power law function like  $\tau \sim R^{-s}$  can effectively describe the dependence of relaxation time ( $\tau$ ) on aspect ratio  $R$ . Significantly, this scenario is almost similar to the 'area non-preserving deformation' case. Here also the exponent,  $s$  in power law variation ( $\tau \sim R^{-s}$ ) exhibits a pronounced temperature dependence.

Now we are interested to determine the thermal ( $T$ ) variation of the exponent  $s$ . The value of the exponent  $s$  ( $\tau \sim R^{-s}$ ) has been calculated for a small range of temperatures in the paramagnetic region and the temperature dependence is illustrated in Fig-6. The result is strikingly similar to the previously mentioned 'area non-preserving deformation' case. It shows that the exponent  $s$  linearly decreases with temperature ( $T$ ) and can be expressed as a linear function of temperature i.e.,  $s(T) = aT + b$ . The estimated values of fitting (by linear regression and the fit-statistics) parameters i.e.  $a$  and  $b$  are systematically represented in a tabular form (Table-2) for different dynamics and boundary conditions.

**Table 2**

Dynamical rule	Boundary condition	$a$	$b$	$\chi^2$	DoF
Metropolis	Open	$-1.61 \pm 0.09$	$4.56 \pm 0.22$	0.0001	3
	Periodic	$-2.51 \pm 0.14$	$6.66 \pm 0.32$	0.0003	3
Glauber	Open	$-1.65 \pm 0.05$	$4.68 \pm 0.11$	$4.1 \times 10^{-5}$	3
	Periodic	$-2.52 \pm 0.02$	$6.73 \pm 0.04$	$5.2 \times 10^{-6}$	3

Table 2: Fitting parameters for the exponent  $s$  versus temperature  $T$  plot (Area preserving deformation). I Tikader, O. Mallick and M. Acharyya, Int. J. Mod. Phys. C (2023) (in press).

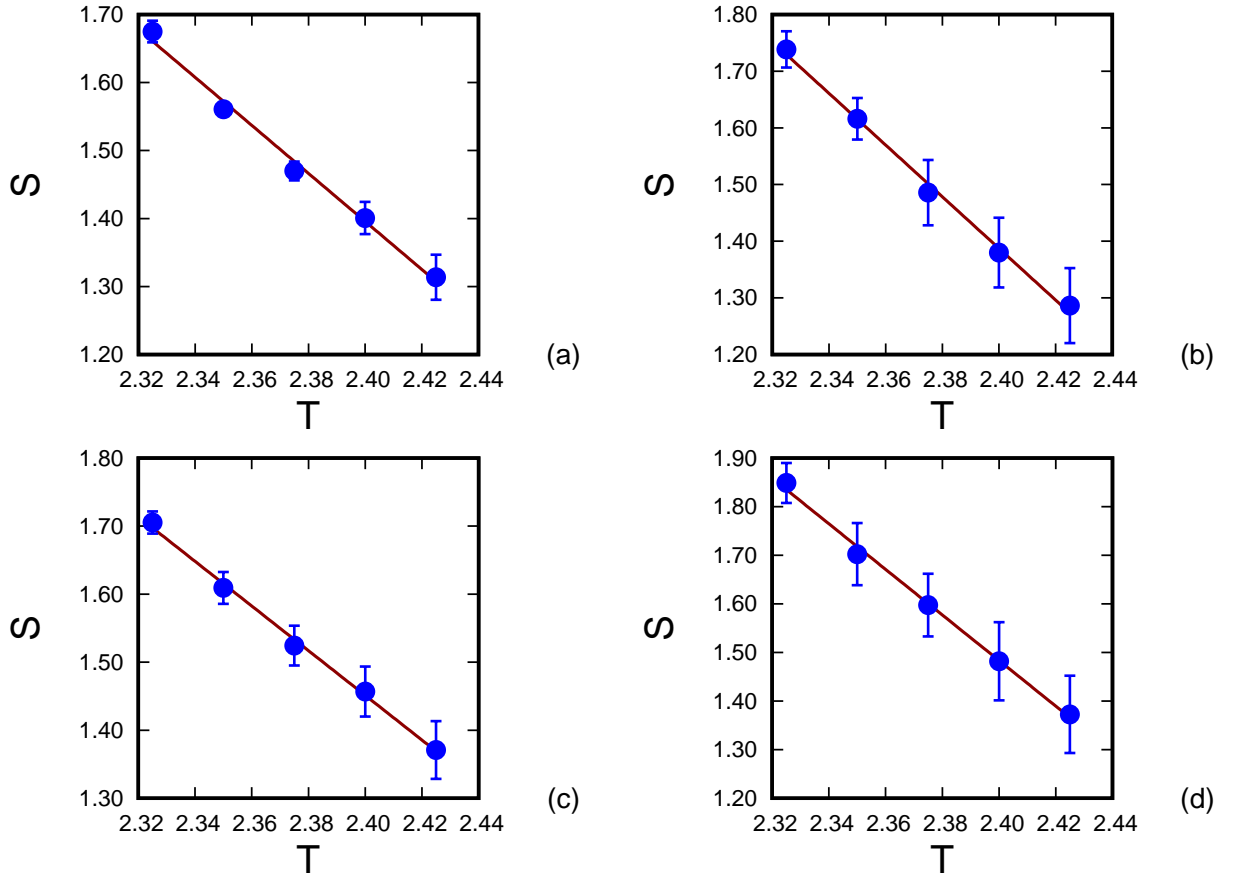


Figure 4: The exponent  $s$  is plotted as the function of the temperature  $T$  (near the critical point, Para phase). The plot is fitted to a straight line function,  $s = aT + b$ . (a) for the open boundary conditions and the Metropolis Algorithm, (b) for the periodic boundary conditions and the Metropolis Algorithm, (c) for the open boundary conditions and the Glauber dynamics and (d) for the periodic boundary conditions and the Glauber dynamics. This figure is collected from the paper authored by I Tikader, O. Mallick and M. Acharyya, arXiv:2212.01858v1.

### 4.1.3 Temporal Growth of Spin flip density

The spin-flip density (the average number of spin-flip per site) is an important measure of the system's relaxation dynamics (Muller-Krumbhaar and Binder 1973) because it reflects the rate at which the system is moving towards its original equilibrium state. A two-dimensional square lattice of size  $L$ , having a total  $N = L^2$  number of spins is considered. The surface of the lattice contains  $N_s = L^2 - (L - 2)^2 = (4L - 4)$  number of spins and the inner part (excluding surface), termed as core contains  $N_c = (L - 2)^2$  number of spins. Starting from the initial configuration where all the spins are pointing up ( $S_i = +1, \forall i$ ), the time evolution of spin-flip density has been studied (Tikader, Mallick and Acharyya 2023) separately for surface and core. As the system relaxes towards its original equilibrium, the corresponding spin-flip density starts to grow with time and eventually saturates at some fixed values after achieving the equilibrium. This saturated spin-flip density (surface/ core) is studied as the function of the system size. Notably, each spin of the core

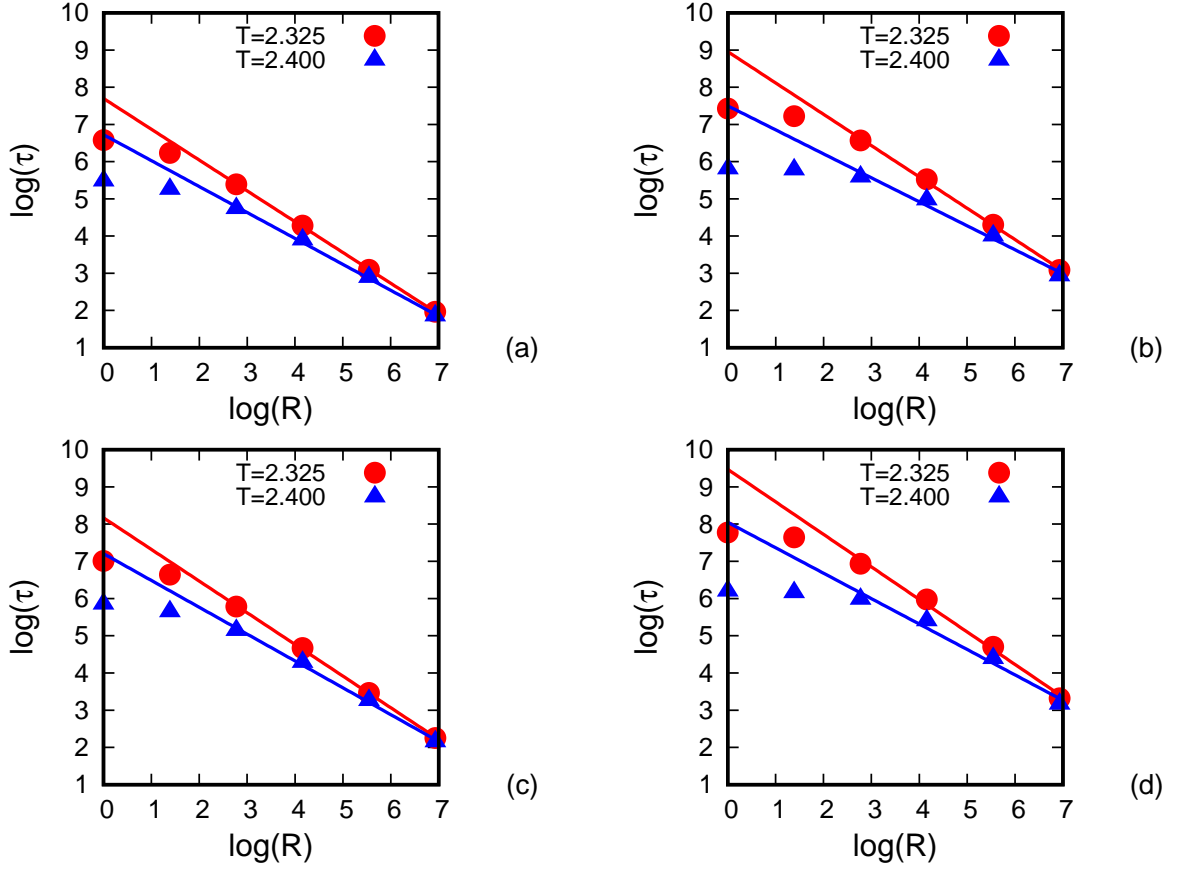


Figure 5: The logarithm of Relaxation time ( $\log(\tau)$ ) is plotted against the logarithm of the aspect ratio ( $\log(R = L_x/L_y)$ ) for two different temperatures in the paramagnetic phase,  $T = 2.325$  (Red circle) and  $T = 2.400$  (Blue triangle). Both are fitted to the straight line,  $\log(\tau) = -s \times \log(R) + r$ . (a) **For open boundary conditions and Metropolis dynamics:** At  $T = 2.325$ ;  $s = 0.827 \pm 0.007$ ,  $r = 7.69 \pm 0.04$  (Red). Here  $\text{DOF}=2$  and  $\chi^2 = 0.001$ . And at  $T = 2.400$ ;  $s = 0.696 \pm 0.022$ ,  $r = 6.72 \pm 0.11$  (Blue). Here  $\text{DOF}=2$  and  $\chi^2 = 0.010$ . (b) **For periodic boundary conditions and Metropolis dynamics:** At  $T = 2.325$ ;  $s = 0.841 \pm 0.022$ ,  $r = 8.95 \pm 0.11$  (Red). Here  $\text{DOF}=2$  and  $\chi^2 = 0.009$ . And at  $T = 2.400$ ;  $s = 0.644 \pm 0.054$ ,  $r = 7.50 \pm 0.27$  (Blue). Here  $\text{DOF}=2$  and  $\chi^2 = 0.056$ . (c) **For open boundary conditions and Glauber dynamics:** At  $T = 2.325$ ;  $s = 0.850 \pm 0.012$ ,  $r = 8.17 \pm 0.06$  (Red). Here  $\text{DOF}=2$  and  $\chi^2 = 0.003$ . And at  $T = 2.400$ ;  $s = 0.721 \pm 0.029$ ,  $r = 7.21 \pm 0.15$  (Blue). Here  $\text{DOF}=2$  and  $\chi^2 = 0.017$ . (d) **For periodic boundary conditions and Glauber dynamics:** At  $T = 2.325$ ;  $s = 0.874 \pm 0.050$ ,  $r = 9.47 \pm 0.25$  (Red). Here  $\text{DOF}=2$  and  $\chi^2 = 0.047$ . And at  $T = 2.400$ ;  $s = 0.683 \pm 0.075$ ,  $r = 8.05 \pm 0.38$  (Blue). Here  $\text{DOF}=2$  and  $\chi^2 = 0.107$ . This figure is collected from the paper authored by I Tikader, O. Mallick and M. Acharyya, Int. J. Mod. Phys. C (2023) (in press).

part interacts with four nearest neighbour spins; while the spin on the edge of the lattice surface can interact with three nearest neighbours and each of the four corner spins can have two nearest neighbours only. In order to study surface relaxation separately, one has to inspect the system with the free surfaces, therefore the open boundary condition is applied to the system.

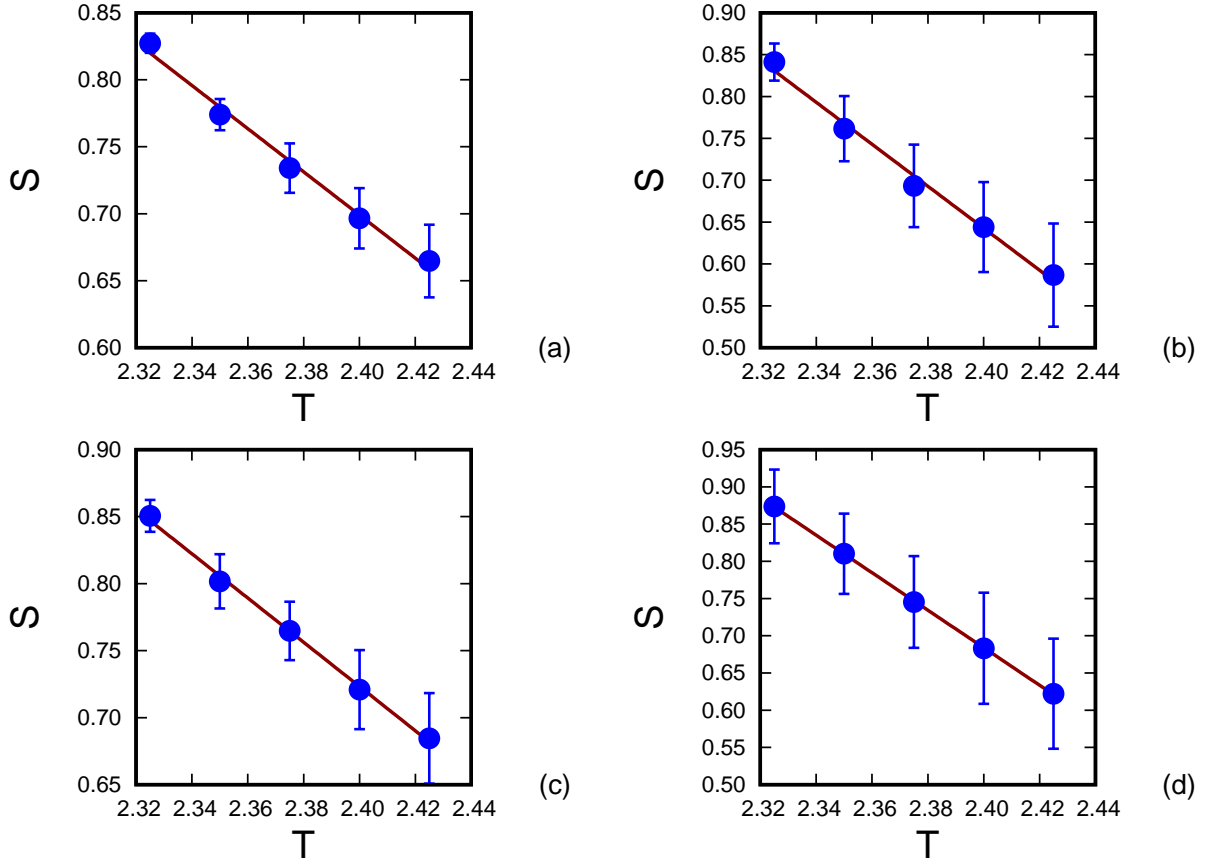


Figure 6: The exponent  $s$  is plotted against the temperature  $T$  (in the paramagnetic phase). The data are fitted to a straight line,  $s = aT + b$ . (a) for the open boundary conditions and the Metropolis algorithm (b) for the periodic boundary conditions and the Metropolis algorithm (c) for the open boundary conditions and the Glauber algorithm and (d) for the periodic boundary conditions and the Glauber algorithm. The values of parameters ( $a$ ,  $b$ ),  $\chi^2$  and degrees of freedom (DoF) are shown in Table 2. I Tikader, O. Mallick and M. Acharyya, Int. J. Mod. Phys. C (2023) (in press) DOI: 10.1142/S0129183123501474.

Here the spin-flip density  $f_d$  is defined as:

$$f_d(t) = \frac{\text{Number of spin-flips(surface/core) at } t^{\text{th}} \text{ MCSS}}{\text{total number of sites on surface/core}} \quad (23)$$

The spin-flip density is obtained by averaging over 10000-80000 different random samples (in accordance with system size). The measurement is done for the system in the ferromagnetic phase ( $T = 2.00$ ) as well as in the paramagnetic phase ( $T = 2.40$ ). Fig-7(a) and Fig-7(b) represent the time evaluation of the core spin-flip density ( $f_d^c$ ) and surface spin-flip density ( $f_d^s$ ) respectively at temperature  $T = 2.0$  using Glauber dynamical rule. It is clearly visible that both core and surface spin-flip density saturates at some steady values after a certain time period. The experiment is repeated for different sizes of lattice ( $L = 200, 100, 50$  and  $25$ ). It is remarkably observed that the saturation values differ with system size  $L$ . The saturated surface spin-flip density ( $f_d^s$ ) is found to be higher than that of the core ( $f_d^c$ ) for a fixed value  $L$ . Similar

studies have been carried out in the paramagnetic region at  $T = 2.4$  also. The evolution of the core and surface spin-flip density with time at  $T = 2.4$  are depicted in Fig-7(c) and Fig-7(d) respectively. Notably, the saturated spin-flip density is quite higher in the paramagnetic phase ( $T = 2.4$ ) for any particular size of the system ( $L$ ). Our observations reveal that the core and surface spin-flip density increase with a decrease in the lattice size ( $L$ ) in both ferromagnetic and paramagnetic regions.

The above-mentioned consecutive simulation studies are again performed, but this time using the Metropolis dynamical rule. The outcomes are qualitatively similar to previous results obtained by using Glauber dynamical rule. However, the results indicate that saturated spin-flip density is notably higher for the Metropolis dynamical rule. The saturated spin-flip density ( $f_d^c$ ,  $f_d^s$ ) is calculated by time averaging

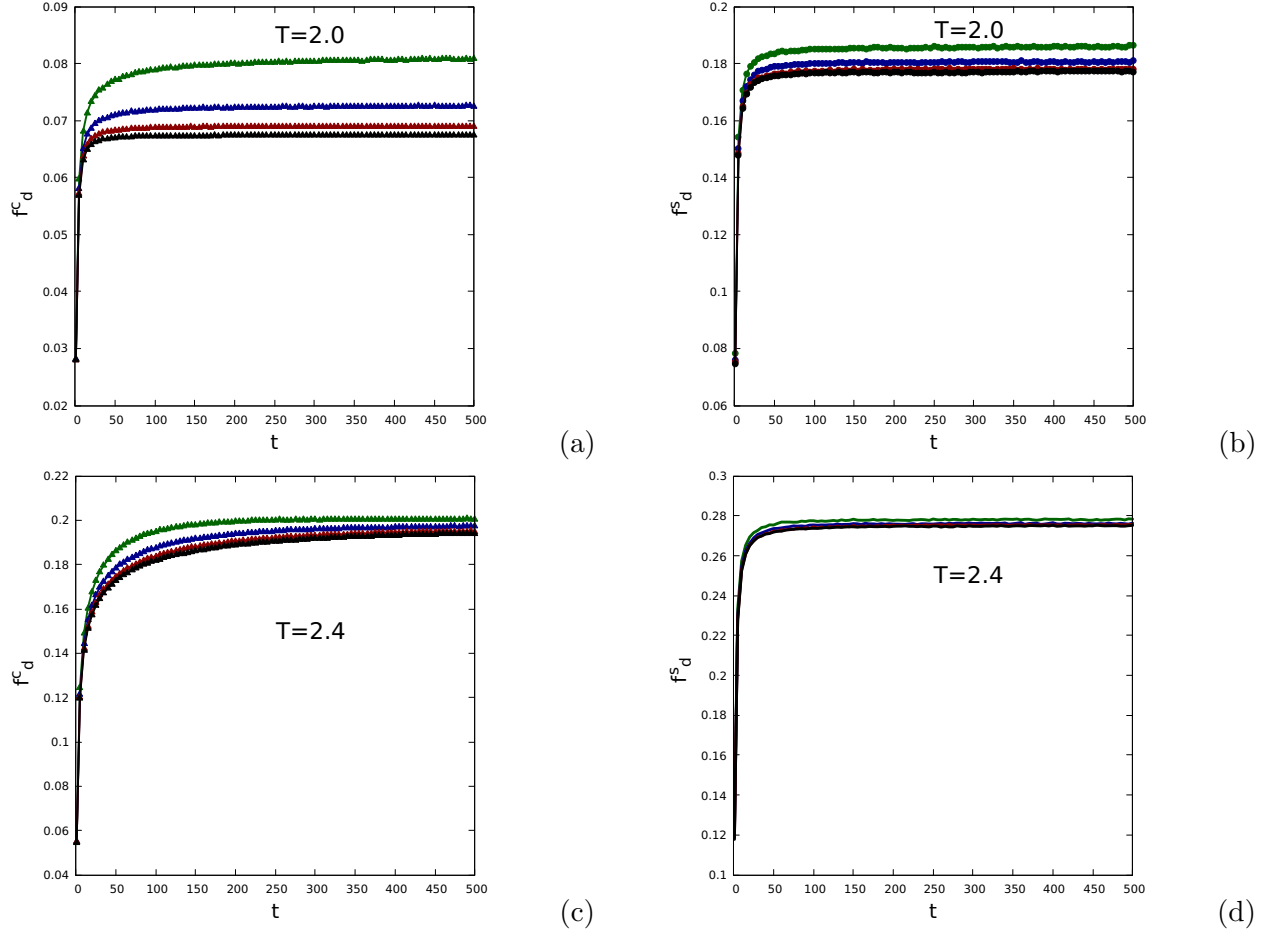


Figure 7: a) Core spin flip density is plotted against the time(MCSS) at the temperature  $T = 2.0$  for different system sizes ( $L$ );  $L = 200$ (black),  $L = 100$ (red),  $L = 50$ (blue),  $L = 25$ (green), (b) Surface spin flip density is plotted against the time(MCSS) at the temperature  $T = 2.0$  for different system sizes ( $L$ );  $L = 200$  (black),  $L = 100$ (red),  $L = 50$ (blue),  $L = 25$ (green), (c) Core spin flip density is plotted against the time(MCSS) at the temperature  $T = 2.4$  for different system sizes ( $L$ );  $L = 200$ (black),  $L = 100$ (red),  $L = 50$ (blue),  $L = 25$ (green), (d)Surface spin flip density is plotted against the time(MCSS) at the temperature  $T = 2.4$  for different system sizes;  $L = 200$ (black),  $L = 100$ (red),  $L = 50$ (blue),  $L = 25$ (green). Here all the results are obtained by using the Glauber dynamics. I Tikader, O. Mallick and M. Acharyya, Int. J. Mod. Phys. C (2023) (in press) DOI:10.1142/S0129183123501474.

ing the spin-flip density over the last 100 MCSS and studied as a function of the system size ( $L$ ). Our results remarked the saturated (core/surface) spin-flip density ( $f_d^c$ ,  $f_d^s$ ) as a linear function of  $\log(L)$ , i.e.,  $f(L) = a + b \log(L)$ . The result is similar for both Glauber and Metropolis dynamics. This analysis is

carried out for both ferromagnetic ( $T = 2.0$ ) and paramagnetic ( $T = 2.4$ ) regions. Here, the results obtained by applying the Metropolis dynamics are demonstrated in Fig-8). Table-2 and Table-4 gives the summarized idea of the fitting parameters and goodness of fit statistics for Glauber and Metropolis dynamics respectively.

**Table 3**

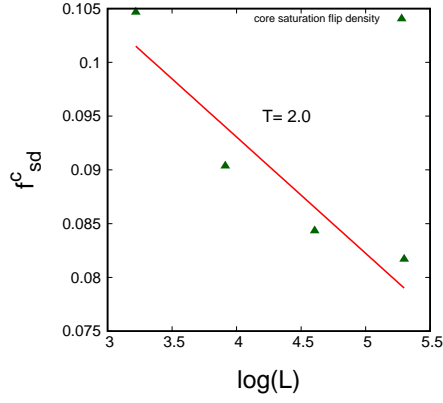
Temperature		a	b	$\chi^2$	DoF
2.0	Core	$0.099 \pm 0.006$	$-0.006 \pm 0.001$	0.000012	2
	Surface	$0.198 \pm 0.005$	$-0.004 \pm 0.001$	0.000005	2
2.4	Core	$0.210 \pm 0.002$	$-0.003 \pm 0.0005$	0.000001	2
	Surface	$0.282 \pm 0.001$	$-0.001 \pm 0.0003$	0.000007	2

Table 3: Fitting parameters for spin-flip density versus logarithm of system size (area preserving deformation). Data obtained by using Glauber Dynamics. I Tikader, O. Mallick and M. Acharyya, Int. J. Mod. Phys. C (2023) (in press), DOI:10.1142/S0129183123501474.

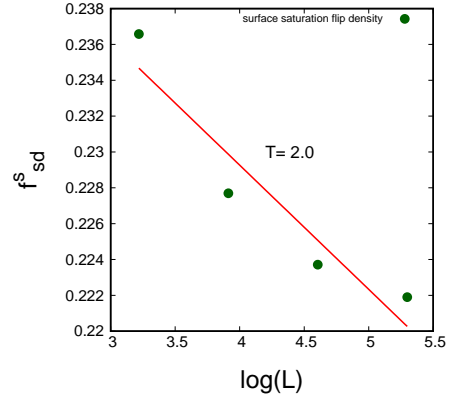
**Table 4**

Temperature		a	b	$\chi^2$	DoF
2.0	Core	$0.136 \pm 0.012$	$-0.011 \pm 0.003$	0.000035	2
	Surface	$0.257 \pm 0.007$	$-0.007 \pm 0.001$	0.000013	2
2.4	Core	$0.308 \pm 0.004$	$-0.005 \pm 0.0009$	0.000003	2
	Surface	$0.385 \pm 0.003$	$-0.0032 \pm 0.0008$	0.000003	2

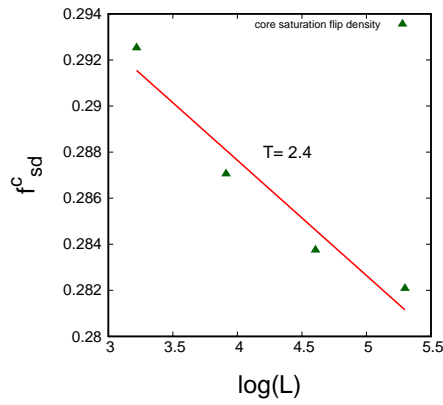
Table 4: Fitting parameters for spin-flip density versus the logarithm of system size. Data obtained by using Metropolis Dynamics. I Tikader, O. Mallick and M. Acharyya, Int. J. Mod. Phys. C (2023) (in press), DOI:10.1142/S0129183123501474.



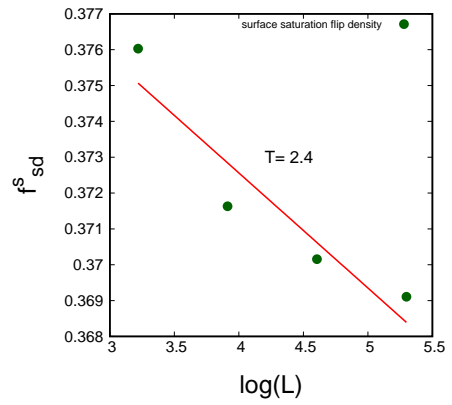
(a)



(b)



(c)



(d)

Figure 8: Plot of saturation spin-flip density versus  $\log(L)$  for core ( $f_{sd}^c$ ) and surface ( $f_{sd}^s$ ) for the temperatures  $T = 2.0$  and  $T = 2.4$ . Data have been obtained by using Metropolis dynamics. The core and surface are labelled as triangles and bullets respectively. Data are fitted to the function  $f(L) = a + b \log(L)$ . The values of coefficients ( $a, b$ ) and  $\chi^2$  are given in Table-4. This figure is collected from the paper authored by I Tikader, O. Mallick and M. Acharyya, Int. J. Mod. Phys. C (2023) (in press) DOI:10.1142/S0129183123501474.

## 5 Experimental results of magnetic relaxation

### 5.1 Critical slowing down

Critical slowing down is a significant phenomenon that occurs in dynamic systems undergoing a second-order phase transition (previously mentioned in Equation 18). The relaxation time  $\tau$  depends on the correlation length  $\xi$  of the fluctuations in the system.  $\tau$  diverges at critical temperature  $T_c$  and satisfies the power-law equation given by (Goldenfeld 1992)

$$\tau(T) = \tau_0 \left[ \frac{\xi(T)}{\xi_0} \right]^z = \tau_0 (\epsilon^{-\nu})^z \quad (24)$$

where  $\nu$  is the critical exponent of diverging correlation length (in 2D Ising Universality class  $\nu = 1.0$ ),  $\epsilon$  is the reduced temperature. Above  $T_c$  it is termed as  $\epsilon = \frac{T-T_c}{T_c}$ .

An experimental study of relaxation behaviour (critical slowing down in particular) in ferromagnetic ultrathin films had been accomplished and power-law scaling of the relaxation time  $\tau$  was observed in the paper Dunlavy and Venus, 2005. In that paper, they measured both (real and Imaginary) components of the complex ac magnetic susceptibility of a two Fe monolayer on W(110) substrate using the surface magneto-optic Kerr effect (SMOKE).

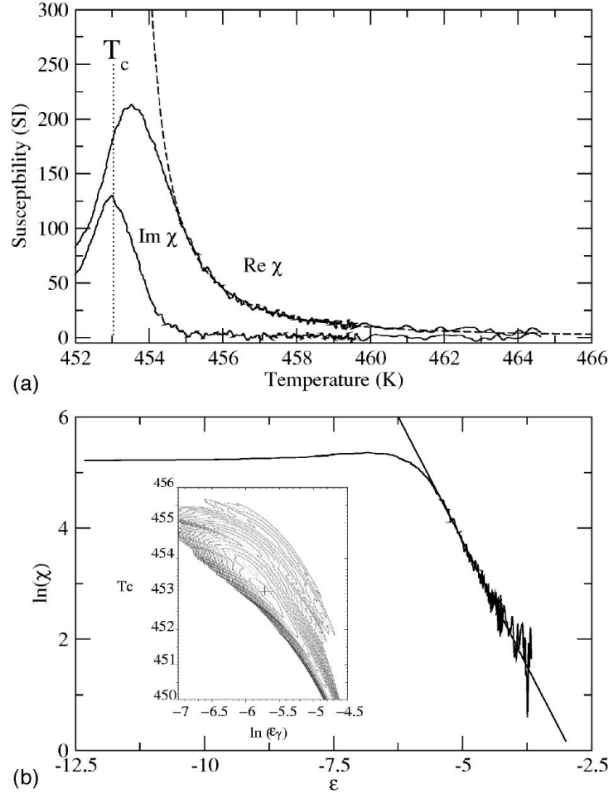
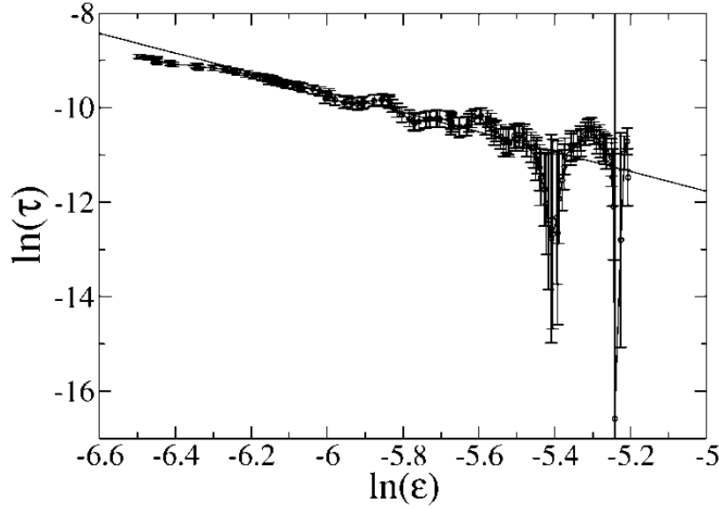


Figure 9: (a) The real and imaginary components of the magnetic susceptibility measured from a two monolayer Fe/W(110) film. The dashed line shows the power-law fit for the real part used to extract the value for  $T_c$  and  $\gamma$ . The dotted line shows the position of  $T_c = 453.03$  K. (b) The real susceptibility in double-log space with the fitted line. The inset figure shows a contour plot of the variance of the fit as a function of  $T_c$  and the cutoff value of  $\ln(\epsilon)$ . The minimum (marked by the cross) shows the best-fit parameters and the fit using those parameters is what is shown by the solid line in (b). The solid contours are separated by the variance levels of  $2 \times 10^{-4}$ . Dunlavy M. J. and Venus D. (2005), Phys. Rev. B 71, 144406.

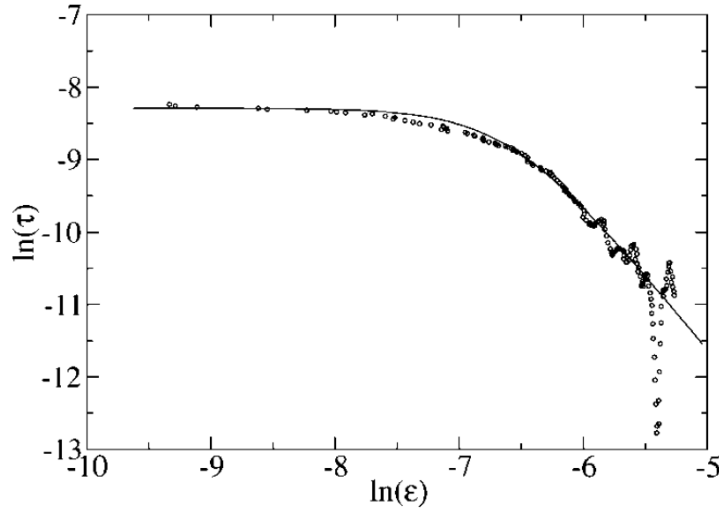
By analyzing the experimental data, the critical temperature of two monolayer Fe/W(110) films is found to be  $T_c = 453.03 \pm 0.02$  K (Figure 9.(a)).

The relaxation time  $\tau$ , measured by the ratio of complex susceptibility, is studied as a function of reduced temperature  $\epsilon$  on a double-log graph, which interprets the power-law scaling of  $\tau$  (Figure 10(a)). From the unbiased statistical analysis the values of both the static critical exponent of susceptibility  $\gamma$  and the dynamic critical exponent  $z$  are determined i.e.  $\gamma = 1.76 \pm 0.06$  and  $z = 2.09 \pm 0.06$  (in 95% confidence limit). The observed results confirm the consistency with the theoretical values (exact results)(Goldenfeld 1992) of the critical exponents for the two-dimensional Ising model.

Further investigation reveals that the power-law behaviour of  $\tau$  only persists closer to critical point  $T_c$  and  $\tau$  eventually saturates due to finite-size and finite-field effects, shown in Figure 10(b).



(a)



(b)

Figure 10: (a) A double-logarithmic plot of relaxation time ( $\tau$ ) as a function of the reduced temperature ( $\epsilon$ ). A linear fit is shown over a small-temperature range between the  $\ln(\epsilon)$  values of  $-6.51$  and  $-5.26$ . The apparent oscillations in the data are artefacts of the low-frequency noise in the data that is magnified on this double-logarithmic scale. (b) A double-logarithmic graph of relaxation time ( $\tau$ ) plotted against the reduced temperature  $\epsilon$ . The solid line shows the fit for  $\xi_{sat}$  using a simple model which includes both power-law scaling and saturation regimes. Collected from Dunlavy M. J. and Venus D. (2005) Phys. Rev. B 71, 144406.

## 6 Summary:

In this article, we have reviewed the published (Tikader, Mallick and Acharyya 2023) results of our Monte Carlo simulational studies on the relaxation dynamics of two-dimensional Ising ferromagnet. Here, mainly the roles of geometry, boundary conditions, and the dynamical rules on the relaxation behavior of Ising ferromagnet, are investigated. The main findings are (i) the exponential relaxation of the magnetisation ( $m(t) \sim e^{(-t/\tau)}$ ). (ii) The relaxation time ( $\tau$ ) has remarkable dependence on the aspect ratio ( $R$ ), in the large  $R$  limit. This is the effect of geometry on the relaxation behaviour. (iii) The power law dependence of the relaxation time ( $\tau$ ) on the aspect ratio ( $R$ ) has been noticed,  $\tau \sim R^{-s}$ . (iv) The exponent ( $s$ ) of the power law has been found to be linearly dependent ( $s(T) = aT + b$ ) on the temperature ( $T$ ) of the system. The above-mentioned observations are universal and found in both (Metropolis and Glauber) kinds of dynamics and for both (open and periodic) types of boundary conditions. It is worth mentioning here that we have observed this power law behaviour both for area-preserving (Tikader, Mallick and Acharyya 2023) and area non-preserving (Tikader, Mallick and Acharyya, 2022, arxiv:2212.01858v1) cases.

For both kinds of deformation (area-preserving and area non-preserving) of the lattice, the values of  $a$  and  $b$  have weak dependence on the dynamical rules and strong dependence on the boundary conditions. The magnitudes of  $a$  and  $b$  are higher for the periodic boundary conditions. The values of  $a$  and  $b$  are provided in a tabular form in Table-1.

The relaxation of the magnetisation in two dimensional Ising ferromagnet (or model magnetic monolayer) depends on the dynamical rules and the geometrical boundary conditions employed in the Monte Carlo simulation. The faster relaxation was observed for open boundary condition irrespective of the dynamical rules (Metropolis/Glauber) employed here. Similarly, Metropolis algorithm yields faster relaxation irrespective of the applied boundary condition (open or periodic). Since the microscopic dynamics responsible for the relaxation behaviour is the spin-flip, we have also studied the temporal growth of instantaneous spin-flip density (already defined in the text). The boundary conditions, used here, are kept open to investigate the behavior in the bulk and on the surface of the system. The reason behind it is just to keep the surface exposed to the environment. However, the behavior of the spin-flip density has been studied both in the ferromagnetic and paramagnetic regions. The behavior of spin-flip density has also been investigated for different (Metropolis and Glauber) dynamical rules. Interestingly, a logarithmic dependence ( $f_d = a + b \log(L)$ ) has been observed for saturated spin-flip density with system size ( $L$ ), both for core and surface. The logarithmic dependence has been observed both in ferromagnetic and paramagnetic regimes also. The values of  $a$  and  $b$  (for such logarithmic fitting) and the values of  $\chi^2$  are given in Table-2 and in Table-3 for Glauber and Metropolis dynamics respectively. All these results are reported recently (Tikader, Mallick and Acharyya, 2023).

This study is an appeal to the experimentalist for further investigation in real magnetic thin film or monolayers. The *magnetic coating* on non-magnetic substrate may show such kind of behaviour. In real life application, the geometrical shape of *magnetic coating* (in credit cards) may be varied to have faster relaxation for quicker response.

## 7 Acknowledgements:

IT acknowledges UGC, Govt. of India for financial support. MA thankfully acknowledges the FRPDF Grant from Presidency University, Kolkata. We thank Olivia Mallick for fruitful collaboration.

## 8 References

- Binder K., Stauffer D. and Muller-Krumbhaar H., 1975, Theory for the dynamics of clusters near the critical point. I. Relaxation of the Glauber kinetic Ising model, *Phys. Rev. B* 12, 5261
- Brey J. and Prados A., 1996, Low-temperature relaxation in the one-dimensional Ising model, *Phys. Rev. E* 53, 458
- Chiesa A., Cugini F., Hussain R., Macaluso E., Allodi G., Garlatti E., Giansiracusa M., Goodwin C. A. P., Ortu F., Reta D., Skelton J. M., Guidi T., Santini P., Solzi M., Renzi R. De, Mills D. P., Chilton N. F., and Carretta S., 2020, Understanding magnetic relaxation in single-ion magnets with high blocking temperature, *Phys. Rev. B*, 101, 174402
- Collins M. F., Collins A. M. Collins and Fahnle M., 1987, Exponents far from  $T_c$  for the relaxation in the kinetic Ising model, *Phys. Rev. B* 35, 394
- Dunlavy M. J. and Venus D., 2005, Critical slowing down in the two-dimensional Ising model measured using ferromagnetic ultrathin films, *Phys. Rev. B* 71, 144406
- Erdem R., 2008, Magnetic relaxation in a spin-1 Ising model near the second-order phase transition point, *J. Magn. Magn. Mater.*, 320, 2273
- Glauber R. J., 1963, Time-Dependent Statistics of the Ising Model, *J. Math. Phys.* 4, 294
- Godfrin H., Frossati G., Herbal B., Thoulounze D., 1980, SURFACE MAGNETIC RELAXATION - RELATION TO  $^3\text{He}\uparrow$  EXPERIMENTS. *Journal de Physique Colloques*, 41 (C7), pp.C7-275-C7-280. DOI: 10.1051/jphyscol:1980742. jpa-00220180
- Goldenfeld N., 1992 *Lectures on Phase Transitions and the Renormalization Group* (Addison-Wesley Publishing Co., MA
- Grassberger P. and Stauffer D., 1996, Stretched and non-stretched exponential relaxation in Ising ferromagnets, *Physica A*, 232, 171
- Gu L. and Wu R., 2020, Origins of Slow Magnetic Relaxation in Single-Molecule Magnets, *Phys. Rev. Lett.*, 125, 117203
- Jeong D., Choi M. Y., and Park H., 2005, Slow relaxation in the Ising model on a small-world network with strong long-range interactions, *Phys. Rev. E* 71, 036103
- Klein O, Charbois V., Naletov V. V., and Fermon C., 2003, Measurement of the ferromagnetic relaxation in a micron-size sample, *Phys. Rev. B*, 67, 220407(R).
- Lin Y. and Wang F., 2016, Linear relaxation in large two-dimensional Ising models, *Phys. Rev. E* 93, 022113
- Majumdar S. N. and Dean D. S., 2002, Slow relaxation in a constrained Ising spin chain: Toy model for granular compaction, *Phys. Rev. E* 66, 056114
- Melin R., 1996, Magnetic field relaxation in ferromagnetic Ising systems, *J. Magn. Magn. Mater.*, 162, 211
- Metropolis N., Rosenbluth A. W., Rosenbluth M. N., Teller A. H., and Teller E., 1953, Equation of State Calculations by Fast Computing Machines, *J. Chem. Phys.* 21, 1087
- Mori Masatoshi, 1993, Monte Carlo simulation of energy relaxation in the two-dimensional Ising model, *Phys. Rev. B* 47, 11499
- Muller-Krumbhaar H. and Binder K., 1973, Dynamic properties of the Monte Carlo method in statistical mechanics, *J. Stat. Phys.* 8, 1
- Muller-Krumbhaar H., Landau and D. P., 1976, Tricritical relaxation in an Ising-Glauber model with competing interactions, *Phys. Rev. B* 14, 2014
- Nowak U. and Usadel K. D., 1989, Monte Carlo studies of slow relaxation in diluted antiferromagnets, *Phys. Rev. B*, 39, 2516
- Oerding K., 1995, Relaxation times in a finite Ising system with random impurities, *J. Stat. Phys.* 78, 893
- Richards P. M., 1969, Theory of Magnetic Relaxation in a Near-Ising System: DyES, *Phys. Rev.* 187, 690
- Rosa J. Calvo-de la Danilyuk A. L., Komissarov I. V., Prischepa S. L. and Tejada J., 2019, Magnetic Relaxation Experiments in CNT-Based Magnetic Nanocomposite, *Journal of Superconductivity and Novel Magnetism*, 32, 3329

- Slichter C. P, 2020, Magnetic relaxation, McGraw-Hill,  
<https://doi.org/10.1036/1097-8542.398200>
- Suran G., Arnaudas J. I., Ciria M., Fuente C. de la, Rivoire M., Chubukalo O. A. and Gonzalez J. M., 1998, Evidences of non-Arrhenius magnetic relaxation in macroscopic systems: Experiments and related simulations, Europhysics Letters, 41, 671
- Suzuki M. and Kubo R., 1968, Dynamics of the Ising Model near the Critical Point. I, J. Phys. Soc. Jpn. 24, 51
- Tikader I., Mallick O. and Acharyya M. 2023, Effects of geometry, boundary condition and dynamical rules on the magnetic relaxation of Ising ferromagnet, Int. J. Mod. Phys. C (in press),  
DOI:10.1142/S0129183123501474
- Tikader I., Mallick O. and Acharyya M. 2022, arxiv:2212.01858v1
- Tomita H. and Miyashita S., 1992, Statistical properties of the relaxation processes of metastable states in the kinetic Ising model, Phys. Rev. B 46, 8886
- Tomita Y. and Nonomura Y., 2018, Critical nonequilibrium cluster-flip relaxations in Ising models, Phys. Rev. E 98, 052110
- Wang J-S. and Gan C. K., 1998, Nonequilibrium relaxation of the two-dimensional Ising model: Series-expansion and Monte Carlo studies, Phys. Rev. E 57, 6548
- Zazo M., Torres L., Iniguez J., Munoz J. M. and Francisco C. de, 1993, Experimental study on magnetic relaxation in  $YBa_2Cu_3O_7$  by means of a simple inductive technique, Applied Physics A, 57, 239